

# Isospin character of the pygmy dipole resonance in $^{124}\text{Sn}$

J. Endres,<sup>1,\*</sup> E. Litvinova,<sup>2,3</sup> D. Savran,<sup>4</sup> P.A. Butler,<sup>5</sup> M.N. Harakeh,<sup>2,6</sup> S. Harissopoulos,<sup>7</sup>  
R.-D. Herzberg,<sup>5</sup> R. Krücken,<sup>8</sup> A. Lagoyannis,<sup>7</sup> N. Pietralla,<sup>4</sup> V.Yu. Ponomarev,<sup>4</sup> L. Popescu,<sup>6,9</sup>  
P. Ring,<sup>8</sup> M. Scheck,<sup>5</sup> K. Sonnabend,<sup>4</sup> V.I. Stolica,<sup>6</sup> H.J. Wörtche,<sup>6</sup> and A. Zilges<sup>1</sup>

<sup>1</sup>*Institut für Kernphysik, Universität zu Köln, Zùlpicher Straße 77, D-50937 Köln, Germany*

<sup>2</sup>*GSI Helmholtzzentrum für Schwerionenforschung, D-64291 Darmstadt, Germany*

<sup>3</sup>*Institut für Theoretische Physik, Goethe-Universität, D-60438 Frankfurt am Main, Germany*

<sup>4</sup>*Institut für Kernphysik, TU Darmstadt, D-64289 Darmstadt, Germany*

<sup>5</sup>*Oliver Lodge Laboratory, University of Liverpool, L69 7ZE, United Kingdom*

<sup>6</sup>*Kernfysisch Versneller Instituut, University of Groningen, 9747 AA Groningen, The Netherlands*

<sup>7</sup>*Institute of Nuclear Physics, N.C.S.R. Demokritos Athens, GR-15310 Athens, Greece*

<sup>8</sup>*Physik Department, TU München, D-85748 Garching, Germany*

<sup>9</sup>*Belgian Nuclear Research Centre SCK\*CEN, B-2400 Mol, Belgium*

(Dated: March 7, 2022)

The pygmy dipole resonance has been studied in the proton-magic nucleus  $^{124}\text{Sn}$  with the  $(\alpha, \alpha'\gamma)$  coincidence method at  $E_\alpha = 136$  MeV. The comparison with results of photon-scattering experiments reveals a splitting into two components with different structure: one group of states which is excited in  $(\alpha, \alpha'\gamma)$  as well as in  $(\gamma, \gamma')$  reactions and a group of states at higher energies which is only excited in  $(\gamma, \gamma')$  reactions. Calculations with the self-consistent relativistic quasiparticle time-blocking approximation and the quasi-particle phonon model are in qualitative agreement with the experimental results and predict a low-lying isoscalar component dominated by neutron-skin oscillations and a higher-lying more isovector component on the tail of the giant dipole resonance.

PACS numbers: 21.10.-k, 21.60.-n, 24.30.Cz, 25.55.-e

Collective phenomena are a common feature of strongly interacting many-body quantum systems directly linked to the relevant effective interactions. Atomic nuclei also show collective behavior. One example is given by the giant resonances, which have been investigated intensively using different experimental methods, see e.g., [1]. The isovector electric giant dipole resonance (IVGDR) has been the first giant resonance to be observed in atomic nuclei. Ever since it has been of particular interest, because collective  $E1$  response is related to symmetry breaking between neutrons and protons. In recent years, the so-called pygmy dipole resonance (PDR) [2–4], a concentration of electric dipole strength energetically below the IVGDR, has been studied intensively in various nuclei. Within most modern microscopic nuclear structure models, this new excitation mode is related to the oscillation of a neutron skin against a symmetric proton-neutron core with isospin  $T = 0$ ; for an overview see the recent review by Paar *et al.* [5]. Consequently, one expects an increase of the PDR strength approaching isotopes with extreme neutron-to-proton ratios. Experiments on radioactive neutron-rich nuclei seem to support this assumption [6–11]. If this picture holds, the strength of the PDR is related to the thickness of the neutron skin and the density dependence of the symmetry energy of nuclear matter [7, 12]. The PDR thus permits experimental access to these properties. However, more consistent systematic investigations and especially more constraints on the structure of the PDR are mandatory, such as the experiments presented in this Letter, in order to confirm this picture.

Up to now only experiments on stable nuclei allow more detailed investigations of the PDR which yield additional observables in order to understand the underlying structure of this new excitation mode. In nuclear resonance fluorescence (NRF) experiments the systematics of the PDR as well as its fragmentation and fine-structure can be studied [3, 4, 13–19] up to the particle threshold. The mean excitation energy and the summed transition strength  $\sum B(E1)\uparrow$  (of up to 1% of the isovector energy weighted sum rule) show a smooth variation for the investigated nuclei [16]. Different partly contradictory microscopic calculations are able to reproduce the mean properties of the measured photoresponse [3, 20–25].

In order to study the structure of the PDR in greater detail additional experiments with complementary probes are necessary. However, owing to the high level densities and excitations of higher multipolarity in the same energy region the experimental investigation of the PDR using other probes than (real or virtual) photons is very difficult. It has been shown [26–28] that the  $(\alpha, \alpha'\gamma)$  reaction at medium energies provides an excellent selectivity to low-spin states similar to NRF and, thus, represents a powerful tool to study  $E1$  strength. First investigations in the  $N=82$  isotones using this method have indicated, in comparison to photon-scattering experiments, an unexpected splitting of the PDR into two well-separated groups of  $J^\pi = 1^-$  states [27, 28]. The data suggest these two groups of  $J^\pi = 1^-$  states have different underlying structures. While recently an isoscalar-isovector splitting of higher-lying  $E1$  strength in relativistic random-phase approximation cal-

culations for  $^{140}\text{Ce}$  has been reported [29], no theoretical calculations which reproduce the experimentally observed splitting of the PDR, are available so far.

In order to prove that the observed splitting of the PDR is not a unique phenomenon of the  $N=82$  isotones we have extended our experimental studies to the  $Z=50$  isotope  $^{124}\text{Sn}$ . In this Letter we present the results of the  $^{124}\text{Sn}(\alpha, \alpha'\gamma)$  experiment together with calculations performed within the RQTBA and QPM models which are able to qualitatively reproduce the observed splitting of the PDR in  $^{124}\text{Sn}$ . Allowing for the data on  $^{138}\text{Ba}$  and  $^{140}\text{Ce}$ , we prove that the splitting into two groups of states is a general feature of the PDR. Both theoretical calculations predict a low-lying isoscalar component of  $J^\pi = 1^-$  states which is dominated by neutron-skin oscillations and a higher-lying more isovector group of states on the tail of the GDR.

The experiment was performed at the AGOR cyclotron at KVI, Groningen, using a 136 MeV  $\alpha$ -beam and a self-supporting metallic  $^{124}\text{Sn}$  target with a thickness of 7.02 mg/cm<sup>2</sup>. The target was enriched to 96.96 %. For the detection of the scattered  $\alpha$  particles the big-bite spectrometer (BBS) [30] was used, which is equipped with the EuroSuperNova (ESN) light-ion detection system [31]. The BBS was positioned at a central angle of 3.5° with an angular acceptance of 1.5°-5.5°. An array of seven high-purity germanium (HPGe) detectors was used to detect the emitted  $\gamma$  rays in coincidence with the scattered  $\alpha$  particles. For a detailed description of the setup see Ref. [32].

In the data analysis the excitation energy (deduced from the measured energy of the scattered  $\alpha$  particle) is plotted versus the decay energy (obtained from the coincidentally measured  $\gamma$ -ray energies) in a two-dimensional matrix. By applying narrow cuts on this matrix,  $\gamma$  decays into different final states of  $^{124}\text{Sn}$  can be selected such as the ground state or the  $J^\pi = 2_1^+$  state.

The selection of decays into the ground state is very efficient to separate the  $J^\pi = 1^-$  states of the PDR from other excitations. From  $(\gamma, \gamma')$  experiments it is known that  $1^-$  states decay predominantly to the ground state in contrast to states of higher multipolarity. By selecting the decays to the ground state nearly background free  $\gamma$  spectra can be generated showing exclusively decays of  $J^\pi = 1^-$  states for  $E_x > 5$  MeV. This demonstrates the excellent selectivity of the method. Figure 1 shows the ground-state decays as a sum of all HPGe detectors. Each HPGe detector has an energy resolution of about 10-15 keV for  $\gamma$ -ray energies between 4 MeV and 9 MeV. This high resolution allows a state-by-state analysis of each single transition. Following the method presented in Ref. [28] the multipolarity and differential  $\alpha$ -scattering cross section can be obtained for each individual observed excitation. Together with the known excitation energies from the NRF experiment a detailed comparison of these two complementary methods becomes feasible.

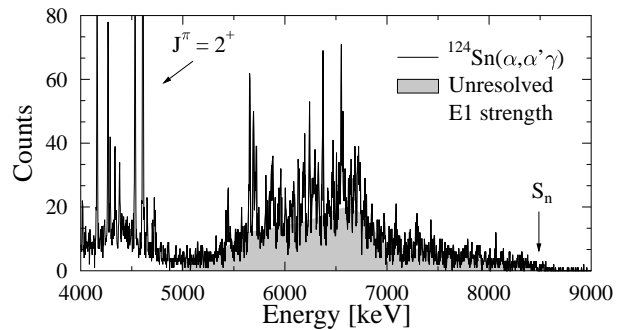


FIG. 1. Summed  $\gamma$ -ray signals of all HPGe detectors after applying the  $\alpha$ - $\gamma$ -coincidence condition for the ground-state decays. The PDR is clearly visible at energies above 5 MeV.

The deduced  $\alpha$ -scattering cross sections for the individual states are presented in Fig. 2(a). The solid line marks the sensitivity limit of the experiment. For comparison, the  $B(E1)\uparrow$  strength distribution measured in NRF is shown in Fig. 2(b). The data have been taken from Ref. [14] and are extended by a recent measurement of some of us where additional states at lower excitation energies have been observed at the high intensity photon setup in Darmstadt [16]. The structure of the spectrum shown in Fig. 1 suggests that strength located in the energy region of the PDR (5.5-9.0 MeV) is not entirely resolved in single transitions, especially above 7 MeV. An analysis of the angular correlation shows that also this part clearly displays a dominant dipole character.

In order to estimate an upper limit of this contribution we calculated the differential cross section in bins of 100 keV width for the complete shadowed part of the spectrum after subtracting the contribution of random coincidences. This integrated cross section is shown in Fig. 3 in comparison to NRF data which represents a lower limit as discussed in Ref. [17]. We also have binned the integrated cross section deduced from the NRF experiment in 100 keV steps. However, it should be stressed that in this case only the cross sections of the single states are included since no contributions from unresolved strength are reported for the photon-scattering experiments.

The comparison of the results of the two experiments [see Figs. 2(a) and 2(b)] shows the same remarkable behavior as already observed in  $^{140}\text{Ce}$  and  $^{138}\text{Ba}$  [27, 28]. Up to a certain excitation energy (about 6 MeV for  $^{140}\text{Ce}$  and  $^{138}\text{Ba}$  and about 6.5 MeV for  $^{124}\text{Sn}$ ) all states which are known from  $(\gamma, \gamma')$  could also be observed in the  $(\alpha, \alpha'\gamma)$  experiments. However, almost all higher-lying states could not be excited with the  $(\alpha, \alpha'\gamma)$  reaction. This abrupt change of response to photons on the one hand and  $\alpha$  particles on the other hand must be related to a structural difference between the group of  $J^\pi = 1^-$  states in the low-energy region and the group of states with higher energies.

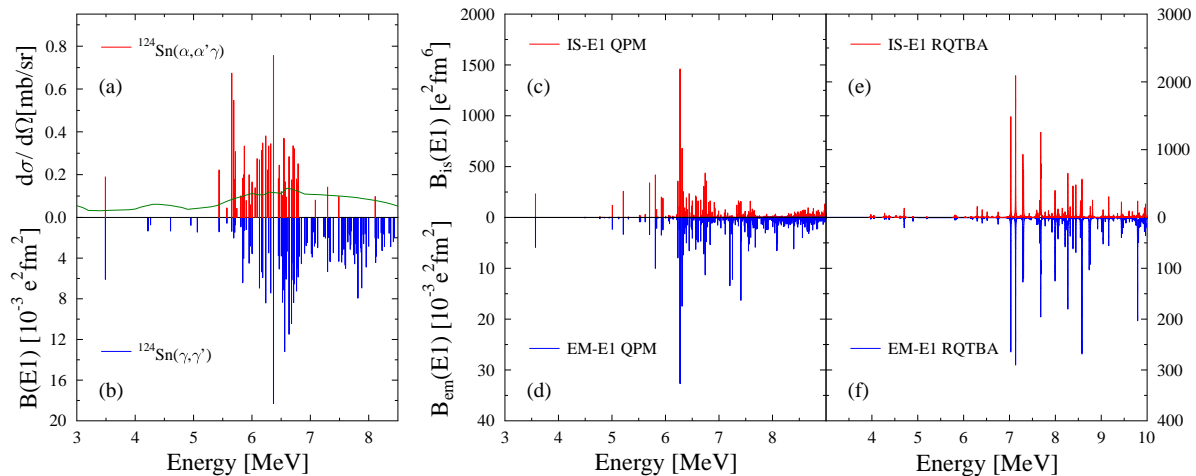


FIG. 2. (a) Singles cross section for the excitation of the  $J^\pi = 1^-$  states in  $^{124}\text{Sn}$  obtained in the  $(\alpha, \alpha'\gamma)$  coincidence experiment. The solid line shows the energy-dependent experimental sensitivity limit. (b)  $B(E1)\uparrow$  strength distribution measured with the  $(\gamma, \gamma')$  reaction. The middle column shows the QPM transition probabilities in  $^{124}\text{Sn}$  for the isoscalar (c) and electromagnetic (d) dipole operators. The RQTBA strength functions in  $^{124}\text{Sn}$  for the isoscalar and electromagnetic dipole operators are shown in (e) and (f), respectively.

This effect has been examined by microscopic calculations. The  $(\gamma, \gamma')$  cross sections can be directly compared to calculated nuclear response to the electromagnetic dipole operator  $r Y_1$ . The calculation of the  $(\alpha, \alpha')$  cross sections involves the Coulomb and nucleon-nucleon terms of the  $\alpha$ -particle interaction with the target nucleus. We have checked that the former term plays a marginal role (less than 10%) under conditions of the present experiment. Then, accounting for a small  $q$  value of the reaction which is about  $0.33 \text{ fm}^{-1}$ , the  $(\alpha, \alpha')$  cross section is proportional with a good accuracy to the response to the isoscalar dipole operator  $r^3 Y_1$ . The spurious center-of-mass motion has been removed (see, e.g., [33] for details).

The nuclear structure part of these calculations has been performed within the quasiparticle-phonon model (QPM) [34] and the relativistic quasiparticle time-blocking approximation (RQTBA) [35], the most representative combination of the microscopic nuclear structure models beyond QRPA. The QPM wave functions of nuclear excited states are composed from one-, two- and three-phonon components. The phonon spectrum is calculated within the quasiparticle random-phase approximation (QRPA) on top of the Woods-Saxon mean field with single-particle energies corrected to reproduce the experimentally known single-particle levels in neighboring odd-mass nuclei. The details of calculations are similar to the ones in Ref. [3, 14, 17]. The results are presented in Fig. 2. Figure 2(d) shows that the electromagnetic strength is strongly fragmented with two pronounced peaks at about 6.3 MeV and 7.5 MeV, in good agreement with the measured  $(\gamma, \gamma')$  data. The

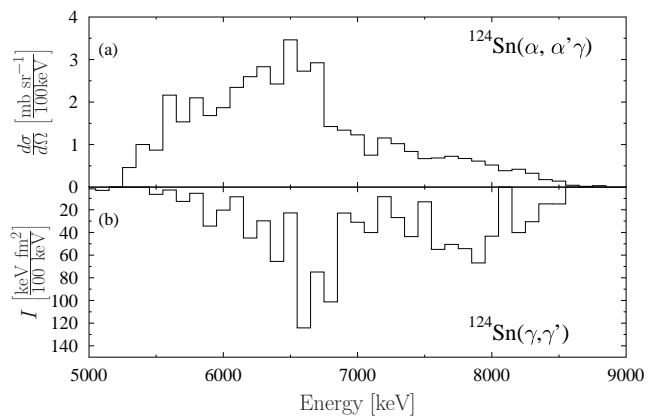


FIG. 3. (a) Differential cross section obtained from the  $^{124}\text{Sn}(\alpha, \alpha'\gamma)$  experiment integrated to bins with a width of 100 keV. (b) Energy integrated cross section measured in  $^{124}\text{Sn}(\gamma, \gamma')$  integrated to bins with a width of 100 keV.

isoscalar response in Fig. 2(c) reveals the suppression of the strength in the higher energy part of the spectrum, in good qualitative agreement with the data.

The RQTBA is based on the covariant energy-density functional and employs a fully consistent parameter-free technique (for details see Ref. [35]) to account for nucleonic configurations beyond the simplest two-quasiparticle ones. The RQTBA excited states are built of the two-quasiparticle-phonon ( $2q \otimes \text{phonon}$ ) configurations, so that the model space is constructed with the quasiparticles of the relativistic mean field and the phonons computed within the self-consistent relativistic QRPA. Phonons of multiplicities  $2^+$ ,  $3^-$ ,  $4^+$ ,  $5^-$ ,

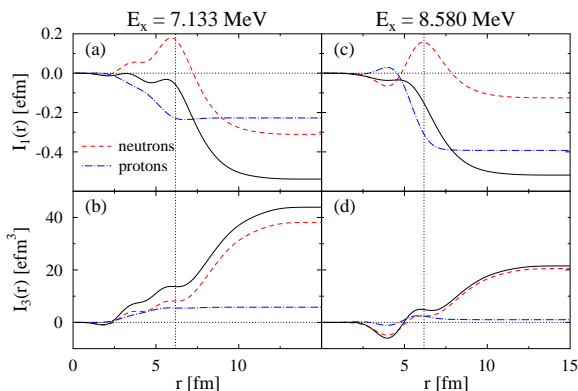


FIG. 4. Electromagnetic  $I_1(r)$  (top) and isoscalar  $I_3(r)$  (bottom) radial integrals for two particular RQTBA states - solid lines. Contribution from neutrons (protons) is shown by dashed (dot-dashed) lines. Vertical dotted line is plotted at the nuclear surface  $R_0 = 1.24 \cdot A^{1/3}$ . See text for details.

$6^+$  with energies below 10 MeV are included in the model space. The result of these calculations is shown in Figs. 2(e) and 2(f). Compared to the experimental and to the QPM spectra, the structural features are shifted by about 600 keV towards higher energies for the  $E1$  electromagnetic strength and even more for the isoscalar dipole strength. Furthermore, the obtained fragmentation is still not sufficient. Nevertheless, the general picture demonstrates clearly the suppression of the isoscalar dipole strength at higher energies.

The PDR pattern of the neutron skin oscillation against the  $T = 0$  core is important in understanding the peculiarities of the reactions under discussion. The RQTBA states at 7.13 and 8.58 MeV have almost equal  $B_{em}(E1)$  but differ in  $B_{is}(E1)$  values by the factor 4. The PDR pattern is well-developed in the first state while contribution from the neutron skin is weaker in the second one. In general, within the RQTBA the deviations from the PDR pattern start to develop above  $\approx 8$  MeV. Fig. 4 plots radial integrals  $I_\eta(r) = \int_0^r \rho_{em(is)}(r) r^{\eta+2} dr$  where  $\rho(r)$  are transition densities;  $\eta = 1$  for electromagnetic and  $\eta = 3$  for isoscalar transitions.  $I_\eta(\infty)$  represents the corresponding transition matrix elements. Notice the dominant role of the external part of transition densities in both electromagnetic and isoscalar cases and its enhancement in the latter due to the higher factor  $\eta$ . While interference of the tails of neutron and proton transition densities plays substantial role in  $I_1(\infty)$ , the  $I_3(\infty)$  quantity is determined by the neutron skin.

This analysis shows that  $\alpha$  particles can be expected to be more sensitive to the surface neutron oscillation mode and less sensitive to states showing stronger contribution of the IVGDR, as expected for the region of the tail of the IVGDR. Therefore, the experimentally observed splitting of the low-lying  $E1$  strength which seems to be a general feature of the PDR suggests, that the low-lying group of

$1^-$  states actually represents the more isoscalar neutron-skin oscillation most often associated with the interpretation of the PDR, while the higher lying  $1^-$  states belong to a transitional region on the tail of the isovector GDR. However, further experimental evidence is desirable to confirm this interpretation, as would be expected from e.g.  $(p, p'\gamma)$  experiments at medium energies.

The presented results show that beside systematic investigation of the PDR with real or virtual photons, experiments on exotic nuclei using isoscalar and surface sensitive probes such as  $\alpha$  particles are one of the most valuable but also most challenging demands to get a deeper understanding of this new excitation mode in atomic nuclei.

This work was supported by the Deutsche Forschungsgemeinschaft (ZI 510/4-1 and SFB 634) and by the LOEWE program of the State of Hesse (Helmholtz International Center for FAIR). The research has further been supported by the EU under EURONS Contract No. RII3-CT-2004-506065 in the 6th framework program, by the DFG cluster of excellence Origin and Structure of the Universe, and by the Russian Federal Education Agency Program. The authors thank P. von Brentano, F. Iachello, H. Lenske, R. Schwengner, and A. Tonchev for stimulating discussions.

\* endres@ikp.uni-koeln.de

- [1] M. N. Harakeh and A. van der Woude, *Giant Resonances* (Oxford University Press, 2001).
- [2] G. A. Bartholomew *et al.*, *Adv. Nucl. Phys.*, **7**, 229 (1973).
- [3] R.-D. Herzberg *et al.*, *Phys. Lett. B*, **390**, 49 (1997).
- [4] A. Zilges *et al.*, *Phys. Lett. B*, **542**, 43 (2002).
- [5] N. Paar *et al.*, *Rep. Prog. Phys.*, **70**, 691 (2007).
- [6] P. Adrich *et al.*, *Phys. Rev. Lett.*, **95**, 132501 (2005).
- [7] A. Klimkiewicz *et al.*, *Nucl. Phys.*, **A788**, 145 (2007).
- [8] T. Aumann, *Nucl. Phys.*, **A805**, 198c (2008).
- [9] J. Gibelin *et al.*, *Phys. Rev. Lett.*, **101**, 212503 (2008).
- [10] O. Wieland *et al.*, *Phys. Rev. Lett.*, **102**, 092502 (2009).
- [11] A. Carbone *et al.*, *Phys. Rev. C*, **81**, 041301(R) (2010).
- [12] J. Piekarewicz, *Phys. Rev. C*, **73**, 044325 (2006).
- [13] N. Pietralla *et al.*, *Phys. Rev. Lett.*, **88**, 012502 (2001).
- [14] K. Govaert *et al.*, *Phys. Rev. C*, **57**, 2229 (1998).
- [15] T. Hartmann *et al.*, *Phys. Rev. Lett.*, **93**, 192501 (2004).
- [16] S. Volz *et al.*, *Nucl. Phys.*, **A779**, 1 (2006).
- [17] D. Savran *et al.*, *Phys. Rev. Lett.*, **100**, 232501 (2008).
- [18] A. P. Tonchev *et al.*, *Phys. Rev. Lett.*, **104**, 072501 (2010).
- [19] R. Schwengner *et al.*, *Phys. Rev. C*, **78**, 064314 (2008).
- [20] E. Litvinova *et al.*, *Phys. Rev. C*, **79**, 054312 (2009).
- [21] N. Tsoneva and H. Lenske, *Phys. Rev. C*, **77**, 024321 (2008).
- [22] A. V. Avdeenkov and S. P. Kamerdzhiev, *Phys. At. Nucl.*, **72**, 1332 (2009).
- [23] N. Paar *et al.*, *Phys. Lett. B*, **606**, 288 (2005).
- [24] G. Colò *et al.*, *Phys. Lett. B*, **485**, 362 (2000).
- [25] E. G. Lanza *et al.*, *Phys. Rev. C*, **79**, 054615 (2009).

- [26] T. D. Poelheken *et al.*, Phys. Lett. B, **278**, 423 (1992).
- [27] D. Savran *et al.*, Phys. Rev. Lett., **97**, 172502 (2006).
- [28] J. Endres *et al.*, Phys. Rev. C, **80**, 034302 (2009).
- [29] N. Paar *et al.*, Phys. Rev. Lett., **103**, 032502 (2009).
- [30] A. M. van den Berg, Nucl. Instr. and Meth. B, **99**, 637 (1995).
- [31] H. J. Wörtche *et al.*, Nucl. Phys., **A687**, 321c (2001).
- [32] D. Savran *et al.*, Nucl. Instr. and Meth. A, **564**, 267 (2006).
- [33] N. V. Giai and H. Sagawa, Nucl. Phys., **A371**, 1 (1981).
- [34] V. G. Soloviev, *Theory of Atomic Nuclei: Quasiparticles and Phonons* (Institute of Physics, Bristol, 1992).
- [35] E. Litvinova *et al.*, Phys. Rev. C, **78**, 014312 (2008).